KLOE Note N. 153
20 November 1995

AN ALGORITHM FOR RECONSTRUCTING STRAIGHT TRACKS IN PROTOTYPE 1

M. Primavera, S. Spagnolo

I.N.F.N., Sezione di Lecce

Abstract

The reconstruction algorithm for straight tracks in the "all stereo" geometry of Prototype 1, the full scale prototype of the central KLOE drift chamber, is described. The algorithm has been tested on Monte Carlo simulations of cosmic rays and beam tracks and results are presented and discussed.

1 Introduction

Prototype 1 [1] was built in order to study the performances of a chamber with all stereo wires arranged in almost square cell, close to the final design of the KLOE experiment tracking chamber, of which it represents a full length cylindrical sector. The most relevant geometrical parameters of the detector are the inner and the outer radii, respectively of 25 and 109 cm, the half aperture of the conical end plates of $80°$, the full length at the inner radius of 290 cm. The prototype has 30 layers of cells, assembled in three different regions. The inner one consists of 10 layers with a cell size of $(1.5 \times \pi/2)\ cm^2$ and an inward displacement at the center of the wire, due to its stereo configuration (stereo drop), of 1 cm. The same drop is in the intermediate section, made of 10 more layers with a cell size of $(3 \times \pi)\ cm^2$. In the outer section, 10 layers of cells of the same size of the previous one, but with a drop of 2 cm, simulate at a smaller radius the stereo angle configuration of the outer layers of the final KLOE chamber (see fig. 1).

A dedicated tracking algorithm has been developed in order to reconstruct straight line tracks either coming from cosmic rays or from beam test data. The main advantage in having a stereo chamber is that a 3$-$dimensional view of the track can be reconstructed globally by using only the wire geometrical parameters. However the pattern recognition is complicated, with respect to an axial or an axial-stereo chamber, by the fact that there is no transverse cross section in which the track view is easily obtained as the tangent to the hit projection in that plane. The pattern recognition algorithm has been designed keeping in mind these two basic facts.

In this note, the track identification and fitting procedures are firstly described, then results obtained on Monte Carlo are presented, in order to evaluate the performances of the reconstruction program.

2 The tracking program

The final goal of the tracking program is to reconstruct straight trajectories inside Prototype 1. The global reference frame is defined, according to the general KLOE frame [2], as shown in fig. 1. The program reconstructs straight line segments, which are described by 6 parameters: the three cartesian coordinates of a generic point P_0, belonging to the track segment, and the three components of a unitary vector $\vec{u}$ which defines the track direction. In this parametrization the equation of the track is:

$$\begin{aligned} x(\theta) &= x_0 + u_x\theta \\ y(\theta) &= y_0 + u_y\theta \\ z(\theta) &= z_0 + u_z\theta \end{aligned} \tag{1}$$

In a single event the information coming from the detector is an array of hit wires. For each of them the DAQ reads a drift time t_j^{meas}, which is translated into a drift distance d_j^{meas} by means of a time to space relation. The track parameters can be obtained by searching for the minimum of a χ^2 function defined as follows:

$$\chi^2 = \sum_{j=1}^{N_{hits}} \left(\frac{d_j^{track}(\alpha_i) - d_j^{meas}}{\sigma_j} \right)^2 \tag{2}$$

where $d_j^{track}(\alpha_i)$ is the distance of closest approach of the $j-$th hit wire to the track with parameters α_i, and σ_j is the uncertainty on the measured drift distance d_j^{meas}. Since the hit

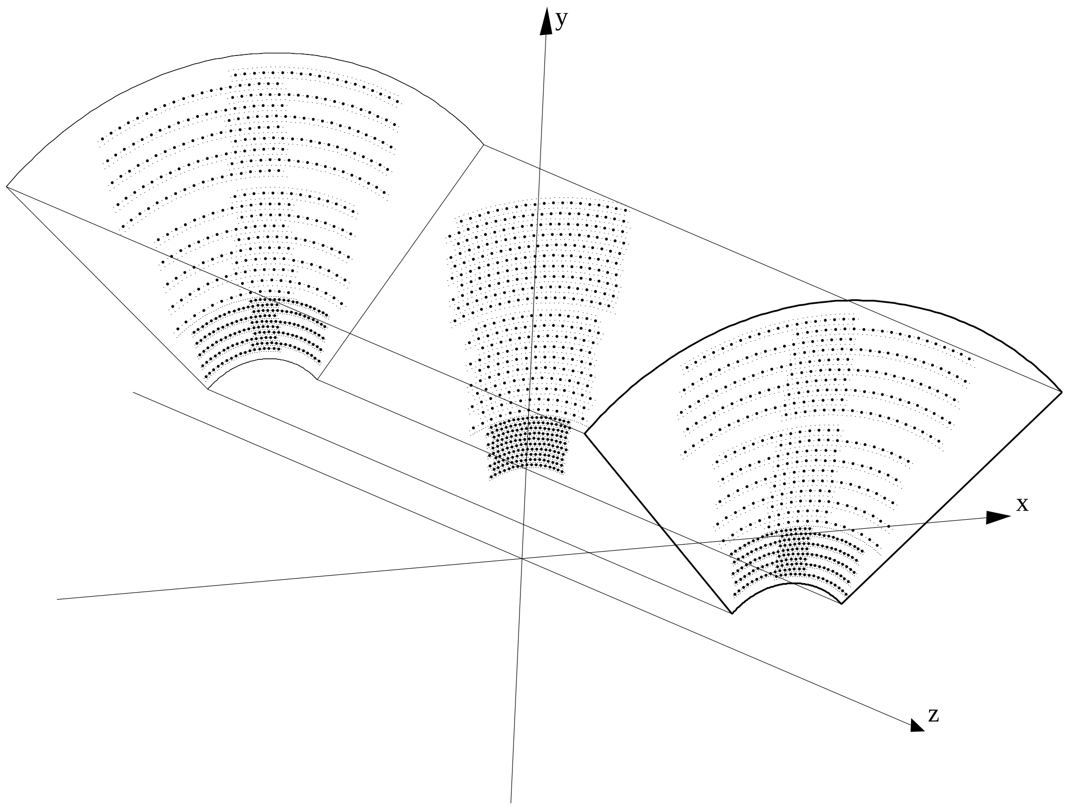

Figure 1: A 3-d view of Prototype 1.

wires are not parallel to each other, the χ^2 in eq. (2) carries a 3−dimensional information about the track. It is a non linear function of the track parameters α_i and there is no analytic solution for the point of minimum. Moreover, all numerical procedures to find the minimum depend in a critical way on the search starting point. These considerations led us to use a standard routine for the χ^2 minimization and to develop a specialized algorithm for the pattern recognition and the track parameters estimate, which could provide reasonably precise starting conditions for a fast convergence of the minimization routine.

3 The track fit procedure

Since the track is a three dimensional straight line, only four of the six parameters which appear in eq. (1) are independent. As a consequence of the adopted parametrization, it is possible to freely choose one of the three coordinates of the point P_0 within a reasonable expected range of variation. We set arbitrarily x_0 or y_0 and we choose the one which, according to the geometrical configuration of the track, makes easier the search for the point P_0 corresponding to the minimum χ^2. [1]

[1] For example, in case of tracks nearly parallel to the y axis, y_0 is fixed because small variations of its value result in even smaller x_0 and z_0 variations, while, for a given x_0, y_0 can range in a large interval

The requirement to have $||\vec{u}|| = 1$ is a further constraint which reduces the number of degrees of freedom in the parameter space. If one of the $\vec{u}$ components is computed as a function of the remaining two, only 4 free parameters survive.

The χ^2 minimization is performed with the gradient method by using MINUIT [3]. This routine provides the coordinates of the point of minimum and the error matrix. If the algorithm doesn't converge, the search restarts with the simplex method and, as soon as a candidate minimum is found, the gradient method is applied in order to compute the error matrix.

The starting parameters for the χ^2 minimization come from the pattern recognition routine, which just uses the hit distribution inside the chamber. Alternatively, the program can provide as input to MINUIT external information. For example, in the cosmic ray stand configuration the planes of RPC, defining the trigger, can provide the coordinates of two points outside Prototype 1 belonging to the track or, in a test beam setup, the orientation of the detector with respect to the beam gives a rough estimate of the track parameters. Since the pattern recognition algorithm requires only 5 consecutive hit layers, only in very special cases the program resorts to these external informations.

4 The pattern recognition algorithm

4.1 General description

In axial chambers, the transverse projection of the track can be defined by the condition of tangency, in the transverse plane, to the circles with centre at the hit wire location and radius corresponding to the drift distance. In Prototype 1 instead, the 3−dimensional track must fullfil the requirement of being tangent to the set of cylinders whose axis coincide with the hit wires and radii are equal to the drift distance.

Two foundamental considerations arise:

- there is no transverse plane in which all sections of the drift cylinders appear to be tangent to the projection of the track;
- once the transverse view of the track is reconstructed, the longitudinal view is obtained by looking at its orientation with respect to the projection of the hit sense wires in the $x - y$ plane.

Taking into account these considerations, the pattern recognition algorithm is developed in two consecutive steps, corresponding to the determination of the transverse $(x - y)$ and the longitudinal $(x - z)$ projection of the track.

4.2 $X - Y$ view

In the simple case of a straight line perpendicular to the z axis, the pattern of hits resembles that of an axial chamber. When the angle between the track and the z axis is different from 90°, in every plane perpendicular to z only the hit profiles close to the intersection P of the track with the plane are approximately tangent to the track projection. Their distance from the track increases with their distance from P (fig. 2).

In order to overcome this difficulty, an axial-like pattern of hits is recontructed in a fictitious transverse plane. This plane is built by projecting the different sections of

without relevant changes in the χ^2 values.

Figure 2: Different transverse sections of a track with a large slope in the $x - z$ plane. The circles represent the hit pattern in the given section, while the square represents the intersection of the track with the section.

pairs of hits, belonging to consecutive layers, each taken in the transverse plane where the distance between the two hits is minimum.

Since each pair of wires has stereo wires of opposite sign, the z coordinate of this plane is a first approximation of the z of closest approach of the track to each of the two hits.

Four pairs of hits or at least five consecutive hits give redundancy to construct the $x - y$ view of the track. This task is performed in the following way:

1. each hit profile in the plane is approximated with a circle at center in the wire location and radius equal to the drift distance;

2. each pair of hits defines four segments tangent to both circles and three points: P_L in the middle of the segment tangent to the left, P_R in the middle of the segment tangent to the right and P_C, the crossing point between the remaining two segments (see fig.3);

Of course, only one of the three points belongs to the transverse projection of the track we are looking for (within the errors coming from the intrinsec resolution of the detector, the circle approximation and, most of all, the approximation in the determination of the z section for each hit).

When four triplets of points (P_L, P_C, P_R) are defined, the twofold ambiguity is removed by searching for the aligned combination of points with a linear fit.

At this stage, an approximate determination of the transverse view of the track is available for the next step: the $x - z$ view reconstruction.

4.3 $X - Z$ view

As already explained, a single hit appears as a cylinder in space tangent to the track. The intersection of the cylinder with a transverse plane located at the z of closest approach

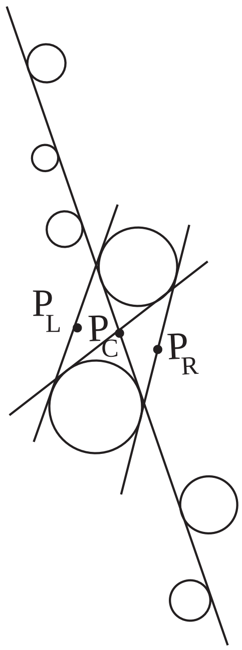

Figure 3: Hit pattern in the fictitious $x-y$ plane

of the hit wire to the track, together with the projection of the track and the projection of the hit wire in this plane, gives an ellipse tangent to the track and with centre on the projection of the hit wire. The equation of the ellipse is easily obtained from the drift distance and from the director cosines of the wire.

Then, given the $x-y$ view of the track and the geometrical arrangement of the hit sense wires, it is possible to define, with a twofold ambiguity, the z of the point of closest approach to each wire by looking at the two ellipses with centres on the wire projection and tangent to the $x-y$ track projection on its left or on its right. A doublet of points, Q_{left} and Q_{right}, is thus associated to each hit and the $x-z$ view of the track is reconstructed by solving the left-right ambiguity by applying an alignement constraint with a linear fit in the $x-z$ plane.

It should be stressed that this algorithm is fully analytic and it works exactly if we provide an exact transverse projection of the track. Monte Carlo tests show that, in this ideal condition, failures in the left-right assignement may occur only in the case of very small drift distances, because of the intrinsic uncertainty on the drift path length.

4.4 Construction of the track candidate

When the first track segment is reconstructed in both views, the following steps are executed for all the hits available in the detector:

a) the next hit in the array is included in the $x-y$ fictitious plane, choosing, as z of the cross section, the longitudinal coordinate of the point of closest approach of the hit wire to the current determination of the track. This defines a new triplet of points (P_L, P_C, P_R);

b) if one of the points in the triplet is compatible, according to a linear fit, with the $x-y$ view of the track, it is added to the track, otherwise the program returns to the point a);

c) the procedure described in section (4.3) is applied to the new hit, the twofold ambiguity (Q_{left}, Q_{right}) is solved and the new point is included in the $x-z$ linear fit, the χ^2 is tested and the hit, eventually, is rejected at this stage even if it has been accepted in the transverse view. In this case the program turns to the point a);

d) the $x-z$ view of the track is used to improve the previous $x-y$ view determination: each transverse profile of the hits is now taken at the z of closest approach of the currently reconstructed track to the hit wire;

When no further hit can be associated to the first candidate track and enough hits are still available, the pattern recognition algorithm starts to build a new track.

5 Monte Carlo event generators

In order to test the track reconstruction program, two different Monte Carlo event generators have been implemented:

a) a naive Monte Carlo, which simulates cosmic rays as straight lines impinging on Prototype 1;

b) a complete GEANT Monte Carlo simulation of cosmic rays and beam particles passing through the detector.

The naive Monte Carlo generates cosmic ray tracks hitting two plane surfaces of size $(300 \times 100) cm^2$, parallel to the $x-z$ plane and placed at $y = 0$ and $y = 200\ cm$ in the prototype reference frame. Then it computes, for each crossed layer, the hit wire as the one closest to the track (only 1 hit per layer is allowed) and the drift distance as the distance of closest approach (DCA). The resolution has been simulated by smearing the drift distances with a gaussian distribution of $\sigma = 200\ \mu m$, constant throughout the cell.

In the GEANT Monte Carlo [4], each cell has been simulated by using a special GEANT active volume ("*polycone*") defined by the coordinates of eight points in space, to take into account the deformation of the cell shape along z. Effects due to multiple scattering, both in the gas and on the sense and field wires have been implemented. In the cosmic ray simulation the particle momentum has been generated according to measured distributions [5], while in the beam simulation it was equal to $140\ GeV/c$ and the beam divergency was $1.4\ mrad$. A prototype resolution of $200\ \mu m$ has been simulated as for the naive Monte Carlo. Differently from the naive Monte Carlo, in which only the cell closest to the track is activated, here all the crossed cells give a hit in the event. A suitable number of tracks can be generated per event and the different effects of the uncorrelated noise can be simulated by choosing the average number of noisy hits to be superimposed to the event.

Both Monte Carlo simulate, in the cosmic ray stand configuration, 6 planes of RPC, instrumented with $3\ cm$ wide strip and aligned with the chamber. A first package of 3 planes is placed above the chamber, while a second is located below the chamber. Each package is equipped with 2 planes of 32 longitudinal (along prototype length) strips, which give the x coordinates and 1 plane of 64 transverse strips, which give the z coordinates. By combining the x and z strips informations, the strip clusters representing the impinging points of the cosmic ray track on the 2 RPC packages can be reconstructed and then the track direction in the space can be determined. No noise has been simulated on RPC detectors.

6 Monte Carlo results

6.1 Cosmic rays

A preliminary test of the track finding capabilities of the described algorithm has been performed by using a sample of 2386 single track noiseless events, produced with the naive Monte Carlo. In this test, all the hits in the event are assumed to belong to the track. The pattern recognition provides a first estimate of the track parameters as input to the track fit procedure and no hit rejection mechanism is applied. Under these conditions, after cutting events with χ^2 probability

$$P(\chi^2) > 0.05 \tag{3}$$

one gets an efficiency of the order of 95%, as expected. In figg. 4 and 5 the χ^2 and the χ^2 probability distributions obtained are shown, together with the distribution of the normalized residues of the drift distance. The sigma of this distribution is slightly smaller than 1, because the track parameters used to compute the DCA of the i-th hit have been determined without removing the hit from the fit. The resolutions on the track parameters, as defined in eq. (1) are given in table 1 and they are fully compatible with the nominal resolution. When the initial track estimate given by the RPC is used, instead of the pattern recognition procedure, the inefficiency of the fitting program (computed as the fraction of the events which pass the probability cut in eq. (3)) increases up $2.4\% \pm 0.3\%$. This is a clear evidence of the higher reliability and quality of the track finding algorithm with respect to the external predictions coming from the RPC.

At the next stage, the hit assignment to the track and the noise rejection procedures have been implemented and tested on 2661 single track Monte Carlo events from the GEANT simulation. When tested on noiseless events, for a very small fraction of these ($0.15\% \pm 0.09\%$) the program reconstructed two tracks and after the probability cut in eq. (3) the reconstruction inefficiency was $1.6\% \pm 0.3\%$. In fig. 6 the normalized distributions of the residues (pulls) of the drift distance and of the coordinates of the point of closest approach to the wire are plotted. As we expect, the z coordinate is more affected by the experimental uncertainties, while the narrow distribution of the y coordinate is explained by the angular distribution of the cosmic ray events. As is observed by comparing figg. 5 and 6a, the resolution on the drift distance becomes slightly worse even in very clean conditions when the hit selection is enabled in the pattern recognition because of a smaller number of hits associated in average to the track.

When uncorrelated noise is superimposed to the event, the probability to reconstruct more than 1 track in the event increases, together with the program inefficiency. In fig. 7 this inefficiency is plotted for a sample of events in which a track with at least eight hits has been reconstructed, as a function of the noise percentage in the detector. As can be observed in this figure, the track reconstruction efficiency drops drastically when the noise occupancy in the event is higher than 5% of the total number of active channels. However, this scenario would correspond, in the case of the KLOE chamber, to

	$\chi^2/d.o.f.$	Mean	Sigma
$x_0^{MC} - x_0^{fit}$ (μm)	50.06/33	0.6 ± 1.6	77.0 ± 1.4
$y_0^{MC} - y_0^{fit}$ (μm)	49.71/50	(34%) 1.16 ± 0.70 (66%) 2.0 ± 1.1	11.2 ± 1.2 38.9 ± 1.5
$z_0^{MC} - z_0^{fit}$ (μm)	44.27/47	16 ± 26	1247 ± 22
$u_x^{MC} - u_x^{fit}$	66.89/45	$(-0.23 \pm 0.45) \cdot 10^{-5}$	$(2.097 \pm 0.040) \cdot 10^{-4}$
$u_y^{MC} - u_y^{fit}$	115.3/58	(48%) $(2.9 \pm 1.1) \cdot 10^{-5}$ (52%) $(-4.8 \pm 3.0) \cdot 10^{-5}$	$(2.45 \pm 0.42) \cdot 10^{-4}$ $(7.78 \pm 0.72) \cdot 10^{-4}$
$u_z^{MC} - u_z^{fit}$	99.78/43	$(-0.9 \pm 4.4) \cdot 10^{-5}$	$(20.28 \pm 0.43) \cdot 10^{-4}$

Table 1: Results on the track parameters in the analysis of the naive Monte Carlo data. Since y_0 and u_y are the most critical parameters in the cosmic ray event configuration, their distributions are better fitted with the sum of two gaussians, whose percent area is specified above together with the mean and the sigma values.

an unrealistic situation in which the detector would be flooded with about 750 noisy hits per event!

6.2 Beam tracks

Events from Monte Carlo beam simulation have been used in order to examine the behaviour of the track finding and fitting program in some critical configurations. When tracks are at small inclination with respect to the x - z plane, the number of fired layers is too small to allow for the pattern recognition to start the track reconstruction, then an external track estimate is required as input to the program (this estimate is given by describing to the program the beam-chamber relative orientation). At this point, the track reconstruction is performed by selecting only hits with a drift distance compatible, within resolution, with the DCA to the track estimate. As an example, results from the program on a sample of 1927 events in which the beam was aligned at an angle of 80° with respect to the y axis are reported here. The area crossed by the beam on the first window surface was of almost 70 cm^2. The χ^2 and χ^2 probability distributions are shown in fig. 8. The inefficiency, which in this case was 3.7%±0.4%, critically depends on the track orientation, and, as expected, the resolution on the track parameters becomes worse as the number of crossed layers in the chamber decreases (e.g. the y_0 parameter is measured within 160 μm and z_0 within 1.5 cm when the beam crosses Prototype 1 at an angle of 80° with respect to the y axis.

7 Conclusions

A track finding algorithm for particles crossing Prototype 1 at $\vec{B} = 0$ has been developed and implemented. Results obtained on Monte Carlo cosmic rays and beam simulation have been found quite satisfactory about the program performances. The program is used to study data collected at CERN beam test during may 1995.

References

[1] The KLOE Collaboration, The KLOE Central Drift Chamber, addendum to the KLOE technical proposal, LNF-94/028 (IR) (1994).

[2] A. Andryakov et al., KLOE note # 115 (1994)

[3] Appl. Soft. Group, CERN Program Library Long Writeup D506 (1992)

[4] G. Cataldi, KLOE note in preparation

[5] M. Aguilar-Benitez et al., Phys. Rev. D50 (1994) 1173

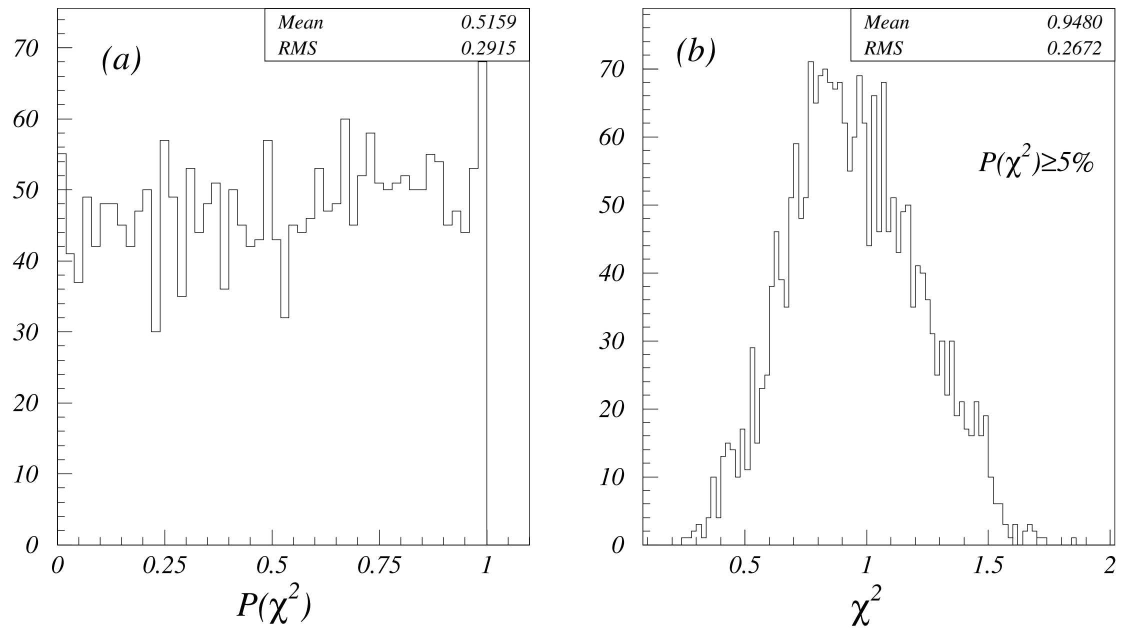

Figure 4: Distribution of χ^2 probability for the whole sample of events from the naive Monte Carlo (a) and χ^2 distribution for the events passing the cut $P(\chi^2) \geq 5\%$ (b).

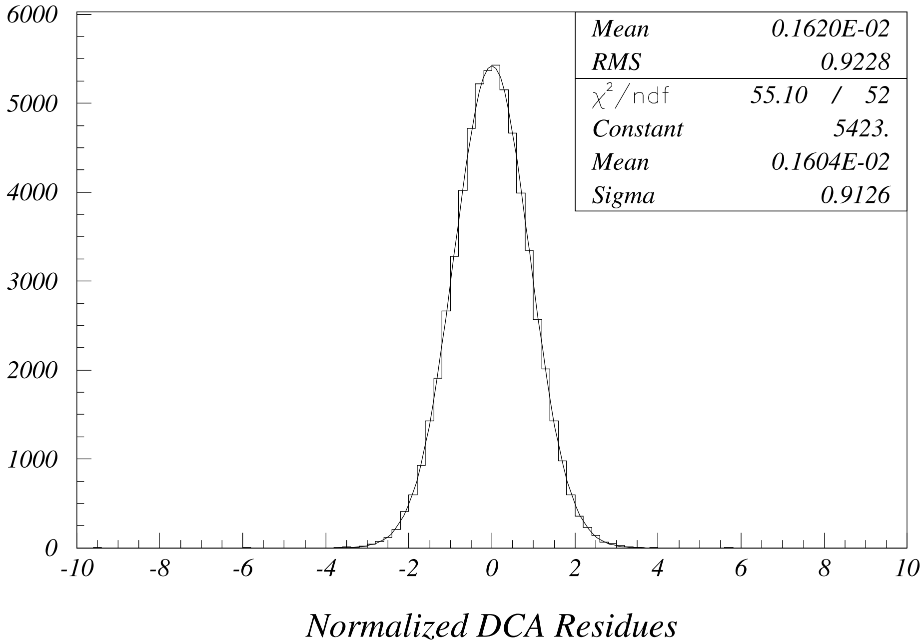

Figure 5: Distribution of the normalized difference between the Monte Carlo generated distance of closest approach (DCA) and the DCA from the reconstructed track. The normalization factor is 200 μm, which is the constant resolution assumed in the track fit procedure.

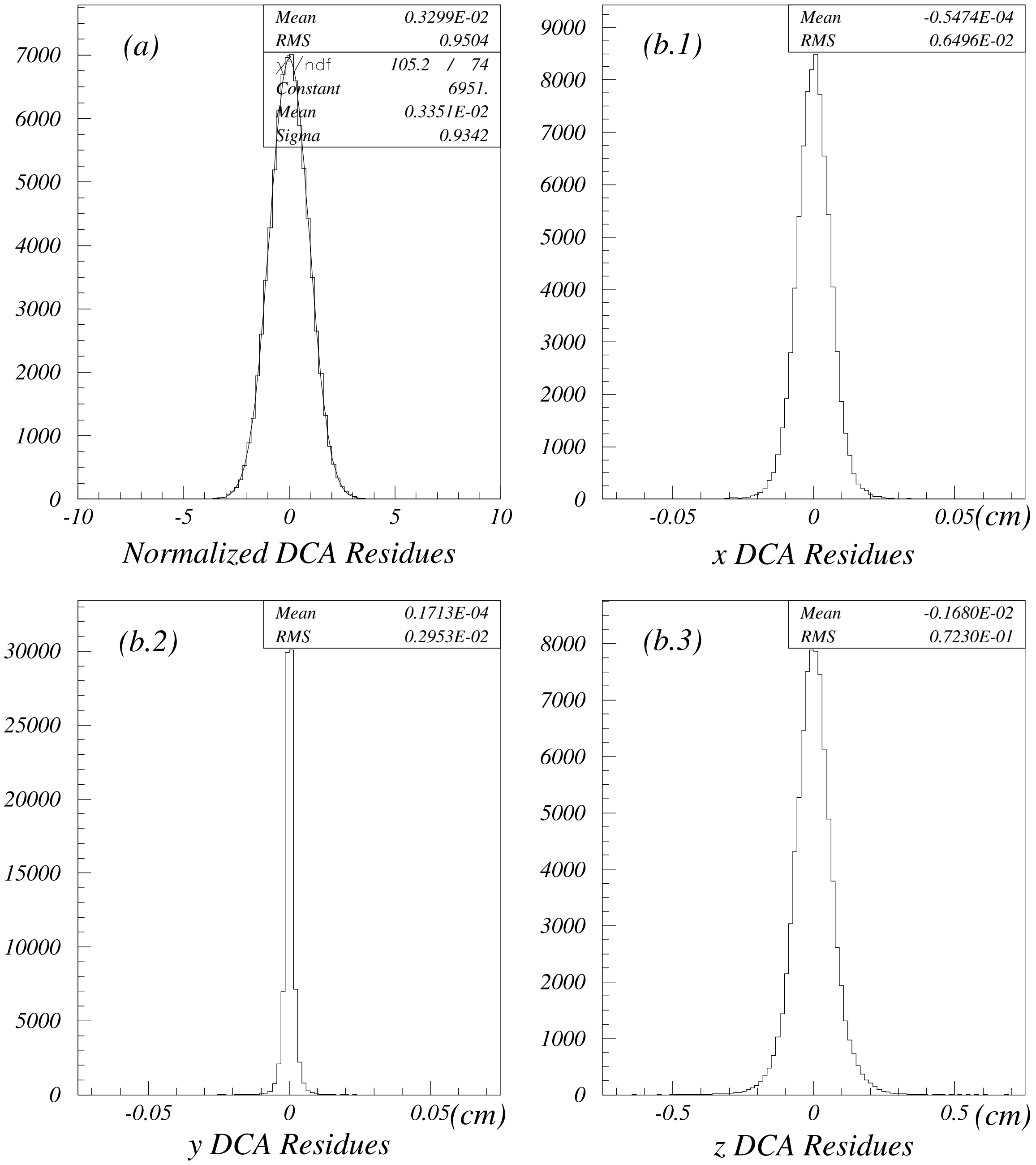

Figure 6: Distribution of the normalized residues (pulls) of the DCA (a) for all the events in the GEANT simulation with $\sigma = 200\ \mu m$. Distributions (b) of the residues on the cartesian coordinates of the points of track-wire closest approach.

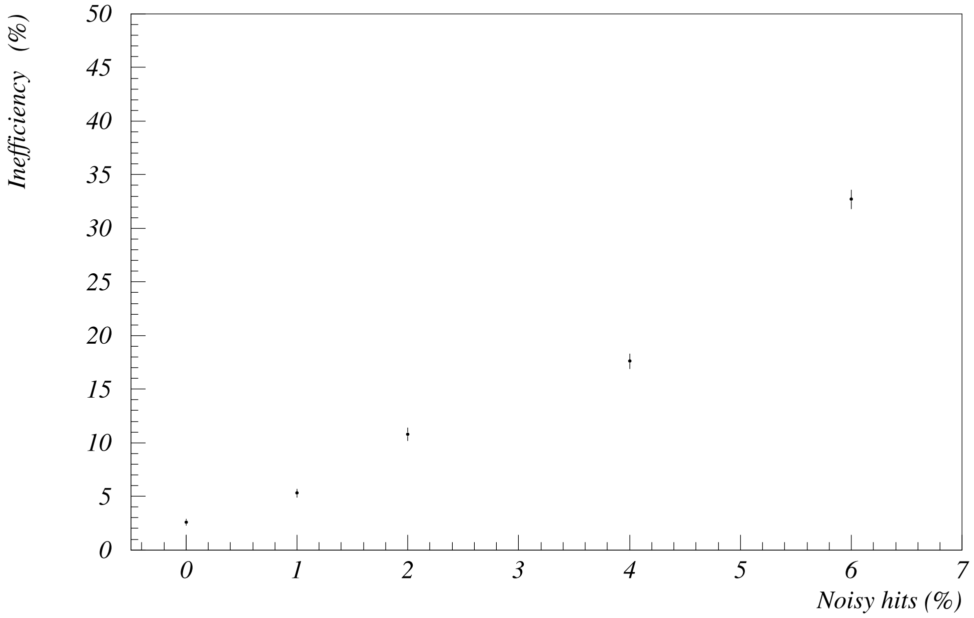

Figure 7: Reconstruction inefficiency versus the number of noisy hits over the total number of cells in the chamber.

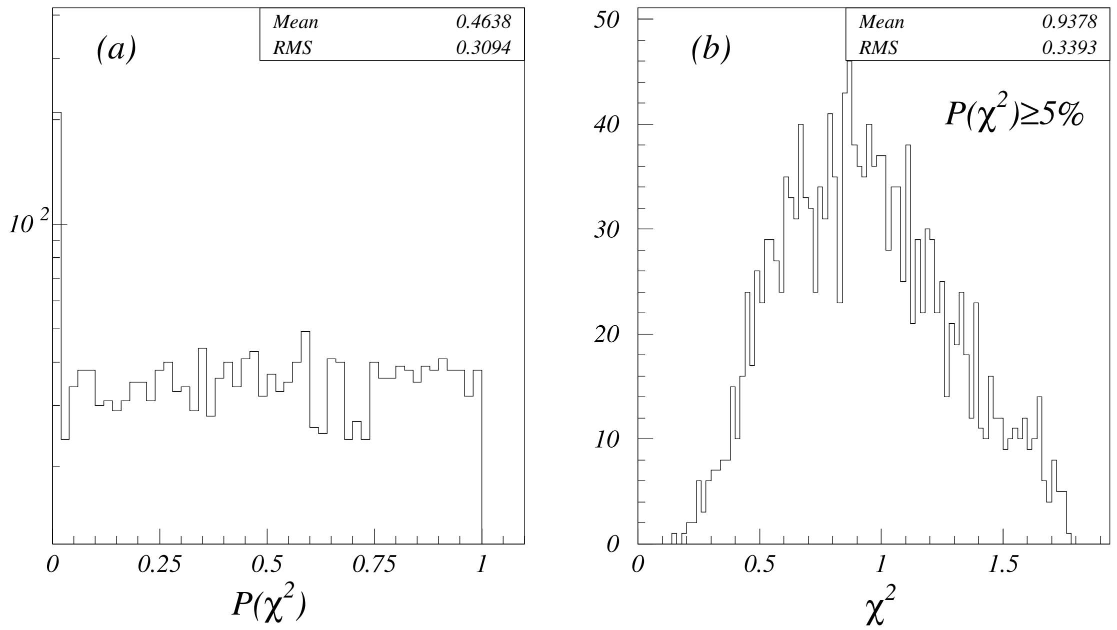

Figure 8: χ^2 probability (a) and χ^2 (b) distributions for events from a simulated beam crossing Prototype 1 at an angle of 80° with respect to the y axis.